Multiscale Compound PDE Approach for Despeckling of US/SAR/OCT Images

S. Kalaivani Narayanan

Abstract—**In this work, a compound PDE approach is proposed in multiscale for speckle reduction of diagnostic Ultrasound (US) images, Satellite aperture radar (SAR) images and optical coherence tomography (OCT) images. In denoising process, it is always difficult to preserve discontinuities in one part of the image and simultaneously recovery of smooth areas in other part of image. Hence, combining different algorithms is the only way to improve the image restoration capability. In this paper, coupled PDE, complex diffusion and second order non linear diffusion are applied to layers 1, 2 and 3 of Laplacian pyramid respectively. . In each pyramid layer, using robust median estimator, gradient threshold is estimated automatically. To limit the number of iterations, mean absolute error (MAE) between two adjacent diffusion steps is used as stopping criteria. Quantitative results on synthetic data and simulated phantom show the performance of the proposed method over state of the art methods. Results on real images demonstrate that the proposed method effectively suppresses the speckle and preserves edges & structural details of the image.**

Index Terms—**Laplacian pyramid, compound PDE, coupled PDE, speckle reduction, multiscale analysis, US image, SAR image, OCT image.**

I. Introduction

Speckle phenomenon is common to laser, sonar, synthetic aperture radar imagery (SAR), optical coherence tomography (OCT) and ultrasound (US) images. Speckle degrades the target detection ability and also reduces the speed and accuracy of post processing tasks such as segmentation and registration etc. Thus, speckle is considered as the dominant source of noise in US/SAR/OCT imaging and should be processed without affecting important image features.

In image despeckling process, the preferred technique should not introduce any blurring effect on the image, and makes no changes or relocation to image edges. Various methods are available in the literature for despeckling [1]-[2], but most of the methods are reducing noise at the cost of smoothing the image and hence softening the edges. To overcome this problem, the partial differential equations (PDEs) –based methods have been introduced in the literature [3]-[4]. An image includes a series of regions in which different regions might have different standard deviations and in despeckling process, it is always difficult to preserve discontinuities in one part of the image and simultaneous recovery of smooth areas in other part of image. Hence, combining different algorithms is the only way to improve the image restoration capability.

Manuscript received May 24, 2012; revised August 31, 2012.

S. Kalaivani Narayanan is with Department of Electronics and Communication Engineering, TRP Engineering College (SRM GROUP), Tiruchirappalli, Tamilnadu, INDIA - 621 105 (e-mail: s_kalai@rediffmail.com, hod.ece@srmtrp.ac.in).

Thus, in this paper, coupled PDE, complex diffusion and second order non linear diffusion are applied to layers 1, 2 and 3 of Laplacian pyramid respectively. The reason for choosing a multi-scale approach is that various sized edges can be filtered properly using both spatial and frequency information. The proposed algorithm is especially efficient for speckle reduction where the noise energy is comparable to the signal energy in a wide range of frequency

II. Background

The basic idea of PDE is to deform an image in a partial differential equation framework and to approach the expected result as a solution to this equation. Diffusion is generally defined as a physical process that equilibrates concentration differences without creating or destroying mass. This physical observation can be easily cast in a mathematical formulation. The equilibration property is expressed by Flick's law:

$$j = -D.\nabla I \quad (1)$$

The diffusion only transport mass without destroying it or creating new mass and is expressed by the continuity equation as,

$$\partial_t I = -div\ \ j \quad (2)$$

If we plug in Flick's law into the continuity equation, we end up with the diffusion equation,

$$\partial_t I = div\ (D.\nabla I) \quad (3)$$

The relation between ∇I and j is described by the diffusion tensor D, a positive definite symmetric matrix.

Second order PDE have studied as a useful tool for image enhancement and scale space analysis of image [3],

$$\begin{cases} \dfrac{\partial I}{\partial t} = \nabla .[c(|\nabla I|)\nabla I] \\ I(t=0) = I_0 \end{cases} \quad (4)$$

where ∇ is the gradient operator, $\nabla.$ is the divergence operator, $\|$ denotes the magnitude, $c(x)$ is the diffusion coefficient and I_0 is the initial image.

Later, the fourth-order partial differential equation is proposed in [4],

$$\frac{\partial I}{\partial t} = -\nabla^2[g(|\nabla^2 I|)\nabla^2 I] \quad (5)$$

The advantage of using fourth-order PDE in image denoising is, it removes the blocky effects that made by

DOI: 10.7763/IJIEE.2012.V2.222

second-order nonlinearity diffusion equation. However, it requires more number of iterations to converge.

Coupled PDE [5] is combination of second order and fourth order PDE that unites the advantages of the second-order and fourth-order PDEs. It avoids the blocky effects caused by second order PDE and it requires only minimum number of iterations compared to fourth order, thus it removes the noise and preserves the edges.

$$\frac{\partial I}{\partial t} = -\nabla.[c(|\nabla I|)\nabla I + c(|\nabla I|)\nabla\nabla^2 I)] \tag{6}$$

A non linear complex diffusion [6] is a process with a complex value diffusion coefficient. In this the imaginary value serves as edge detector, good noise handler and as a controller for non linear process.

$$\frac{\partial I}{\partial t} = -\nabla.[c(\mathrm{Im}(I))\nabla I] \tag{7}$$

Several multi-scale methods based on wavelet and pyramids have been proposed for speckle reduction in ultrasound imaging. The image pyramid offers a flexible and convenient multi-resolution format that mirrors the multiple scales of processing in the human visual system [7]-[8]. The basic classifications of pyramids are: Gaussian pyramid and Laplacian Pyramid. For an input image I , let its Gaussian pyramid at layer l be G_l, and its Laplacian pyramid at layer l be L_l, where $l=0,1,2,.....d-1$ and d is the total decomposition layer. The Gaussian and Laplacian pyramid can be defined as:

$$\begin{aligned} G_0 &= I \\ G_l &= REDUCE \quad [G_{l-1}] \\ L_l &= G_l - EXPAND \quad [G_{l+1}] \end{aligned} \tag{8}$$

The Gaussian pyramid consists of a set of low pass filtered copies of the original image at different sizes, whereas the Laplacian pyramid decomposes the original image into a set of band pass images and a final low pass image.

III. Proposed Multiscale Compound PDE Approach

The proposed multiscale compound PDE (MCP) method consists of four stages as shown in Fig.1.The operations are as follows:

1) Transformation of an image into its Gaussian pyramid domain representation.
2) Transformation of an Gaussian image into its Laplacian pyramid domain representation
3) Manipulation of pyramid coefficients by different PDEs:
   Layer 1: Coupled PDE or Permutated Diffusion
   Layer 2: Complex diffusion
   Layer 3: Second order non linear Diffusion
4) Reconstruction from the diffused Laplacian pyramid.

In the first step an image is decomposed into its pyramid structure of decreasing frequencies.

The second step applies permutated diffusion, complex diffusion and second order non linear diffusion to layer 1, 2, 3 respectively to each band pass layer of Laplacian pyramid to suppress speckle and to preserve edges.

In the first layer that is on L_0 , the permutated diffusion is applied to manipulate the coefficients as,

$$\begin{aligned} &\frac{\partial I(x,y,t)}{\partial t} = -\nabla.[D_1\nabla I(x,y,t) + D_2\nabla I(x,y,t)\nabla^2 I(x,y,t)] \\ &if \quad D_1 = D_2 = c(|\nabla I|) - Diffusion \ \ coeffecien \\ &c(|\nabla I|) = \exp\left(-\left[\frac{|\nabla I|}{k}\right]^2\right) \end{aligned} \tag{9}$$

In the second layer L_1 coefficients are processed by complex diffusion,

$$\begin{aligned} &\frac{\partial I(x,y,t)}{\partial t} = -\nabla.[c(\mathrm{Im}(I))\nabla I] \\ &d(\mathrm{Im}(I)) = \frac{\exp(i\theta)}{1+\left(\frac{\mathrm{Im}(I)}{k\theta}\right)^2}, \quad \theta \in (-\pi/2, \pi/2) \end{aligned} \tag{10}$$

In the third layer L_2 coefficients are manipulated by second order non linear diffusion,

$$\begin{aligned} \frac{\partial I(x,y,t)}{\partial t} &= \nabla.[c(|\nabla I|)\nabla I] \\ c(|\nabla I|) &= \exp[-(\|\nabla I\|/k)^2] \end{aligned} \tag{11}$$

Gradient threshold k in all the three cases is estimated as follows,

$$k(l) = \frac{1}{0.6745}\, median\left(\frac{|\nabla I(l)|}{\sqrt{2\log((l+1)/l)}}\right) \tag{12}$$

where, l represent the pyramid layer and the mean absolute derivative of zero mean normal distribution with unit variance is 0.6745. In the lowest pyramid layer large gradient threshold value is utilized since speckle is dominant. On the other hand, to preserve structure boundaries a small gradient threshold is applied in higher layers.

A. Numerical Implementation

Let the time step be Δt and the spatial step be h in x, y directions. Then the time and space coordinates can be discretized as,

$$\begin{aligned} &t = n\Delta t, n = 0,1,2......., \quad x = ih, y = jh, \\ &i = 0,1,2,.... M-1,\ j = 0,1,2,.... N-1\ \&\ h = 1 \end{aligned}$$

$|\nabla I|$ is discretized as,

$$|\nabla I| = 0.5 \times \sqrt{|\nabla I_N|^2 + |\nabla I_S|^2 + |\nabla I_W|^2 + |\nabla I_E|^2} \tag{13}$$

The image gradients are obtained from directional differences,

$$\begin{aligned} &\nabla I_N^n(i,j) = I_{i-1,j}^n - I_{i,j}^n \ \nabla I_W^n(i,j) = I_{i,j-1}^n - I_{i,j}^n \\ &\nabla I_S^n(i,j) = I_{i+1,j}^n - I_{i,j}^n \ \nabla I_E^n(i,j) = I_{i,j+1}^n - I_{i,j}^n \end{aligned} \tag{14}$$

The Laplacian can be discretized as,

$$\nabla^2 I_{i,j}^n = I_{i+1,j}^n + I_{i-1,j}^n + I_{i,j+1}^n + I_{i,j-1}^n - 4I_{i,j}^n \qquad (15)$$

The diffusion coefficient in (8),(9) & (10) can be calculated using (14).

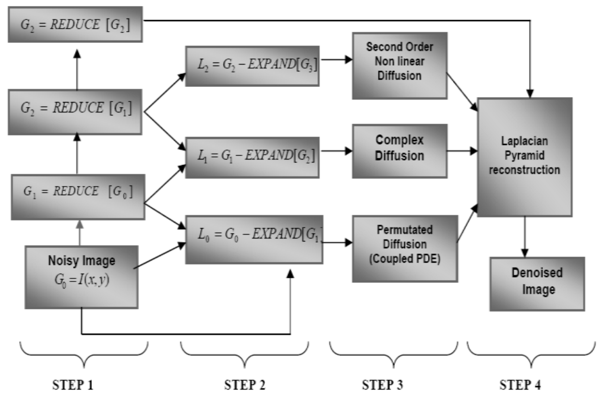

Fig. 1. Block diagram of proposed multiscale compound PDE (MCP) approach

TABLE I: PERFORMANCE MEASURES

Image	For SAR Image		
	FOM	SSIM	MSE
Original	0.125	0.109	106.3
SWWF	0.619	0.694	88.13
LPND	0.802	0.832	93.45
MCP	0.916	0.932	20.87

Image	For OCT Image		
	FOM	SSIM	MSE
Original	0.089	0.184	121.69
SWWF	0.578	0.612	84.85
LPND	0.756	0.802	91.02
MCP	0.924	0.917	16.82

TABLE II: PERFORMANCE MEASURES

Image	For US Image		
	FOM	SSIM	MSE
Original	0.156	0.200	121.43
SWWF	0.703	0.721	86.23
LPND	0.867	0.867	94.65
MCP	0.942	0.924	18.23

B. *Stopping Criteria*

One challenging task in diffusion process is deciding when the iteration is to be stopped. The mean absolute error (MAE) between two adjacent diffusion steps can be used to stop the iteration.

$$MAE(I(t)) = \frac{1}{M \times N} \sum_{(i,j)=1}^{M,N} \sqrt{(I(i,j,t) - I(i,j,t-1))^2} \qquad (16)$$

where *I(i, j, t)* and *I(i, j, t-1)* are the filtered values of the pixel *(i,j)* at time *t* and *t-1*, respectively and *M* , *N* are the numbers of columns and rows in the processed image, respectively.

C. *Image Quality Measures*

To quantify the performance improvement of the proposed MCP approach, three measures are computed. The edge preservation ability is measured using figure of merit (FOM) ,

$$FOM = \frac{1}{\max\{\hat{N}, N_{ideal}\}} \sum_{i=1}^{N} \frac{1}{1 + d_i^2 \lambda} \qquad (17)$$

where N and N_{ideal} are the numbers of detected and original edge pixels, respectively; d_i is the Euclidean distance, λ is a constant typically set to 1/9. Canny edge detector is used to find the edge in all processed results.

Second metric is mean square error in this metric, the smaller the MSE value, the better is the denoising process.

$$MSE = \frac{1}{MN} \sum_{i=1}^{M} \sum_{j=1}^{N} (I_{original}(i,j) - I_{denoised}(i,j))^2 \qquad (18)$$

Third, the structural similarity index (SSIM) is preferred as a quality assessment factor [9] that characterizes the luminance, contrast and structural changes,

$$SSIM(x,y) = \frac{(2\mu_x \mu_y + C_1)(2\sigma_{xy} + C_2)}{(\mu_x^2 + \mu_y^2 + C_1)(\sigma_x^2 + \sigma_y^2 + C_2)} \qquad (19)$$

where, the standard deviation σ_x and the mean intensity μ, covariance σ_{xy} are calculated using local statistics within a total of N windows. Constants $C_1, C_2 << 1$ to ensure stability and N is chosen as 32. The SSIM has values in the 0 to 1 range, with unity representing structurally identical images. The SSIM values are calculated only for simulated images for which the original is available for comparison

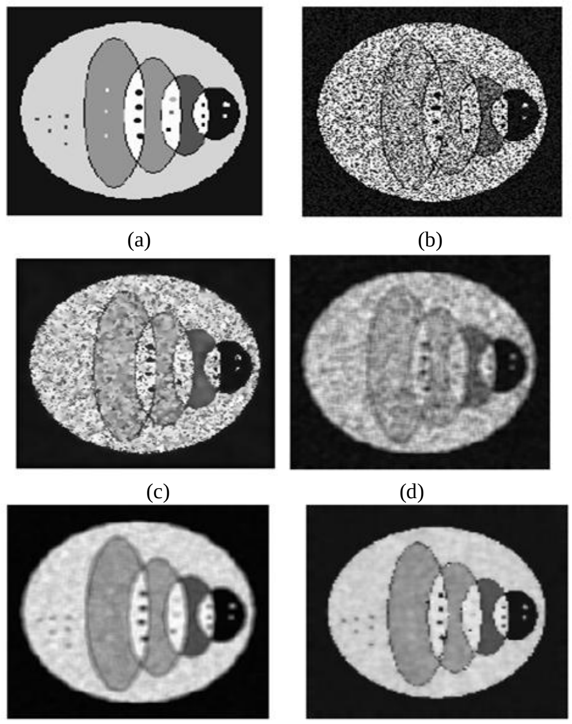

Fig. 2. Result on test image (a) original (b) noisy (c) SWWF (d) LPND (e) H-BM (f) proposed MCP

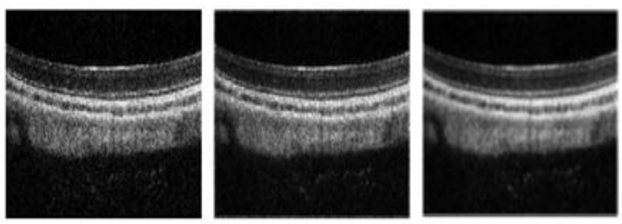

(a) (b) (c)

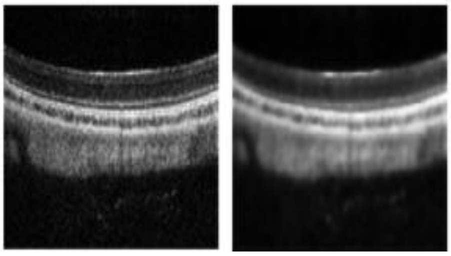

(d) (e)

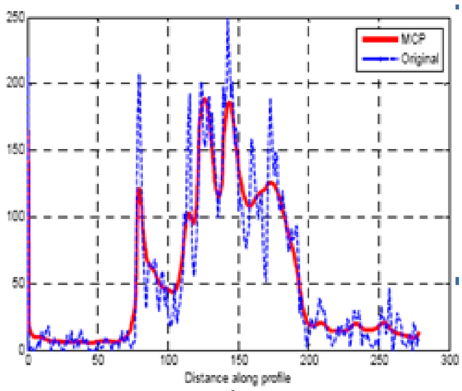

(f)

Fig. 3. Result on OCT image (a) original (b) SWWF (c) LPND (d) H-BM (e) proposed MCP (f) profile along 180th column

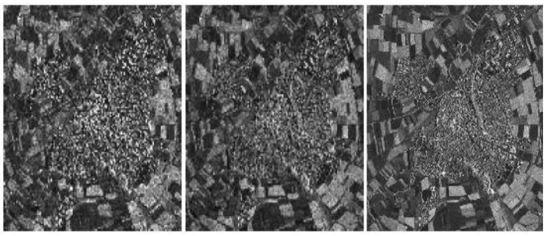

(a) (b) (c)

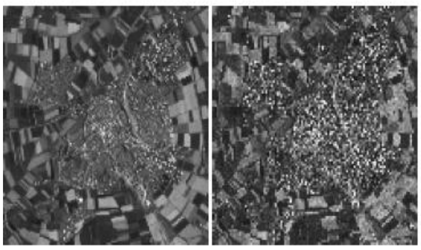

(d) (e)

Fig. 4. Result on SAR image (a) original (b) SWWF (c) LPND (d) H-BM (e) proposed MCP

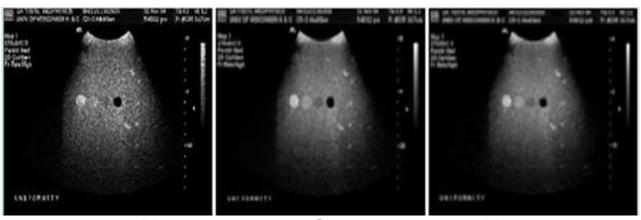

(a) (b) (c)

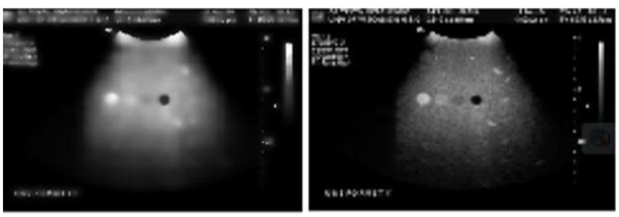

(e) (f)

Fig. 5. Result on US image (a) original (b) SWWF (c) LPND (d) H-BM (e) proposed MCP

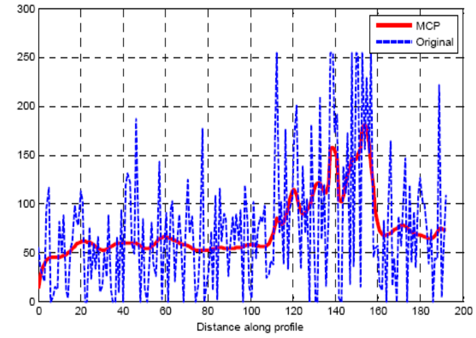

(a)

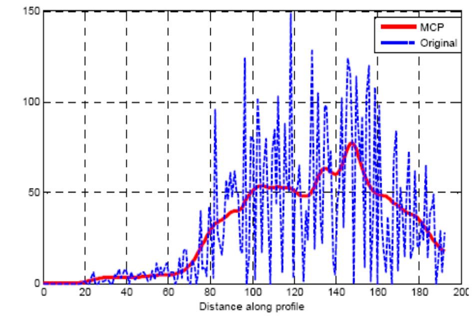

(b)

Fig. 6. Image profile along (a) 131st column in SAR image (b) 800th row image

IV. Experiment Result and Discussion

The performance of the proposed MCP approach is evaluated using artificial image and real US, SAR and OCT images. The results are compared with Laplacian pyramid based non linear diffusion (LPND)[10], stationary wavelet domain wiener filer (SWWF)[11] and homomorphic block matching (H-BM) algorithm [12]. The results on test and real image are depicted in Fig. 2 to 6. Performance of the proposed MCP algorithm and the other state of the art methods on OCT finger skin image, SAR terrace image and real US are listed in table. The table values and the image profile indicate that our proposed MCP model shows advantage over the three methods in terms of speckle reduction, edge preservation and structural detail conservation.

V. Conclusion

In this work, a new multiscale compound PDE approach is proposed for speckle reduction, Speckle is a common issue in US, OCT and SAR images. Moreover, a single algorithm may fail to perform simultaneously the discontinuities and fine details preservation as well as effective speckle reduction. Hence, in this work, three different algorithms are applied to the coefficients of Laplacian pyramid layers depending upon the existence of the degree of speckle. We experiment our proposed MCP method on all three types of images along with a set of test images. The performance of the proposed method is quantified over three recently proposed multiscale methods through different metrics. Experiment results indicate this method has better satisfactory performance in terms of speckle reduction and detail preservation than other methods. Furthermore it can be easily implemented and robust.

REFERENCES

[1] S. K. Narayanan and R. S. D. Wahidabanu, “A view on despeckling in ultrasound imaging,” *Int, Journal on image and video processing*, vol. 2, no. 3, pp.284-294, 2009.

[2] V. Dutt and J. F. Greenleaf, “Adaptive speckle reduction filter for logcompressed B-scan images,” *IEEE Trans. Med. Imag*, vol. 15, no. 6, pp. 802fbv–813, Dec. 1996

[3] P. Perona and J. Malik, “Scale-space and Edge Detection Using Anisotropic Diffusion,” I*EEE Trans. On Pattern Analysis and Machine Intelligence*, vol. l2, pp.629-639, 1990.

[4] Y. L. You and M. Kaveh, “Fourth-Order partial diferential equations for noise removal,” *IEEE Trans. On Image Processing*, vol. 9, pp.1723-1730, 2000.

[5] S. Kalaivani and R. S. D. Wahidabanu, “Diagnostic Ultrasound Image Enhancement- A Multiscale Permutation Approach,” *Journal of Imaging Science and Technology*, vol. 56, no. 1, Jan-Feb 2012.

[6] G. Gilboa and N. Sochen et.al, “Image enhancement and denoising by complex diffusion process,” *IEEE Trans. On Pattern Analysis and Machine Intelligence*, vol. 25, no. 8, pp.1020-36, 2004.

[7] A. L. Alparone, S. Baronti, and F. Lotti, “Multiresolution localstatistics speckle filtering based on a ratio Laplacian pyramid,” *IEEE Trans. Geosci. Remote Sens.*, vol. 36, no. 5, pp. 1466–1476, Sep. 1998

[8] V. P. Melnik, I. Shmulevich, K. Egiazarian, and J. Astola, “Block-median pyramidal transform: Analysis and denoising applications,” *IEEE Trans. Signal Process*, vol. 49, no. 2, pp. 364–372, Feb. 2001.

[9] Z. Wang, X. C. Bovik, H. R. Sheikh, and E. P. S. Celli, "Image quality assessment: From error visibility to structural similarity," *IEEE transactions on Image Processing*, vol. 13, no. 04, pp 1-14, April 2004

[10] F. Zhang, L. M. Koh, Y. M. Yoo, and Y. Kim,“Nonlinear diffusion in laplacian pyramid domain for ultrasonic speckle reduction,” *IEEE Trans. Med. Imag*, vol.26, no.2, pp.200-211, 2007.

[11] S. Solbo and T. Eltoft, “A Stationary Wavelet-Domain Wiener Filter for Correlated Speckle,” *IEEE Trans. Geosci. Remote Sensing*, vol. 46, no. 4, April 2008

[12] S. Parrilli and M. Poderico et.al, “A Nonlocal SAR Image Denoising Algorithm Based on LLMMSE Wavelet Shrinkage,” *IEEE Trans. Geosci. Remote Sensing* ,vol. 50, no. 2, February 2012.